Supporting Information

Quantitative Assessment of Nanoparticle Biodistribution by Fluorescence Imaging, Revisited

Fanfei Meng, Jianping Wang, Qineng Ping, Yoon Yeo

1 Supporting Table

23 Supporting Figures

Supporting Table 1. Size and zeta potential of NPs measured by dynamic light scattering

Dye/NP[1]	Target DiR loading (wt%)	Size (nm)[2]	PDI	Zeta potentials[3] (mV)
$DiR_{0.5}$/np	0.5	184.4 ± 6.9	0.08 ± 0.02	-7.5 ± 1.2
$ICG_{0.5}$/np	0.5	188.9 ± 3.2	0.14 ± 0.14	-13.0 ± 0.5
$DiR_{3.6}$/np	3.6	229.6 ± 8.9	0.09 ± 0.04	-7.7 ± 1.4
$DiR_{0.5}$/np-pTA-pFol	0.5	181.2 ± 6.0	0.06 ± 0.05	-16.3 ± 0.7
$DiR_{0.5}$/np-pTA-PEG	0.5	191.8 ± 15.4	0.09 ± 0.06	-17.1 ± 0.3
$DiR_{3.6}$/np-pTA-pFol	3.6	225.0 ± 28.6	0.05 ± 0.03	-12.4 ± 0.9
$DiR_{3.6}$/np-pTA-PEG	3.6	220.9 ± 31.5	0.09 ± 0.05	-15.5 ± 0.5

[1] NP samples were prepared in bicine buffer (10 mM, pH 7.4).
[2] Size: mean ± s.d., n = 3 independently prepared batches
[3] Zeta potential: mean ± s.d., n = 3 measurements of a representative batch

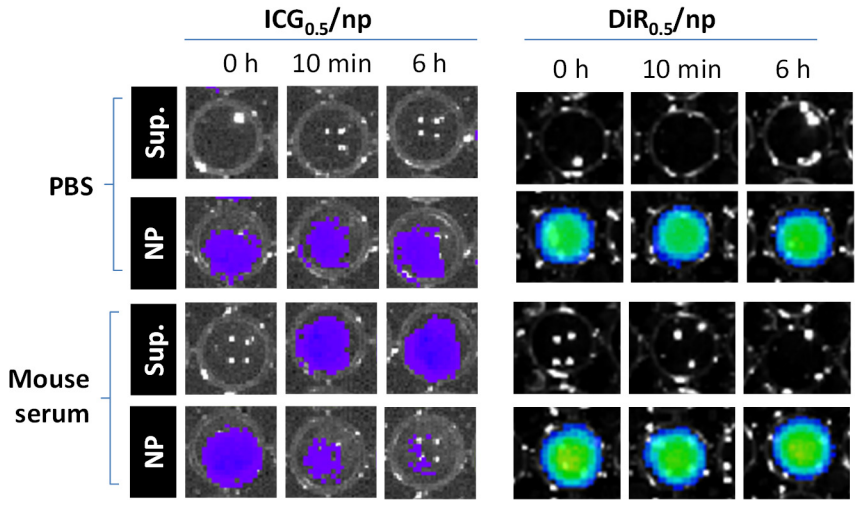

Figure S1. Fluorescence intensity of $ICG_{0.5}$/np and $DiR_{0.5}$/np suspended in PBS and mouse serum, observed at different time points. $ICG_{0.5}$/np or $DiR_{0.5}$/np incubated in mouse serum at 1 mg/mL for the specified time. The supernatant was collected, and the NP pellet was redispersed in fresh mouse serum and imaged by NIR whole body imaging systems. $ICG_{0.5}$/np samples were imaged by IVIS Lumina II Optical Imaging System with an excitation wavelength of 745 nm and an emission filter for ICG, and $DiR_{0.5}$/np samples by a SPECTRAL AMI Imaging System (Spectral Instruments, Tucson, AZ) with an excitation and emission wavelength of 745 and 790 nm, respectively.

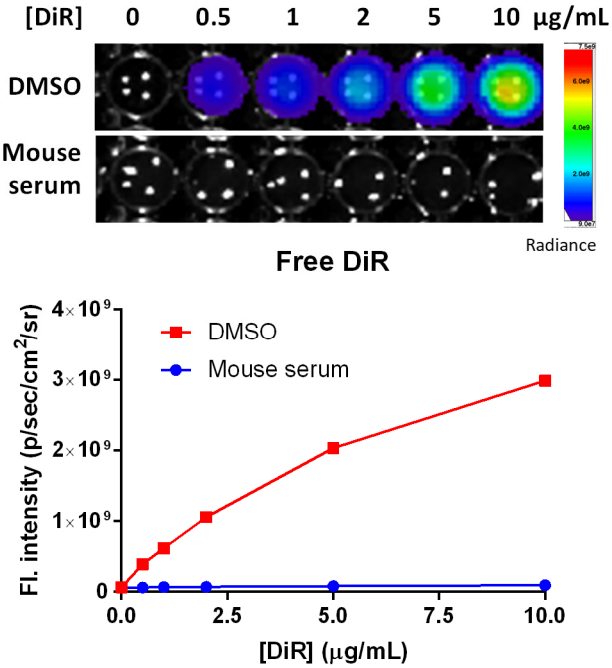

Figure S2. Fluorescence intensity *vs*. concentration of free DiR in DMSO or mouse serum. The fluorescence intensity was quantified by the SPECTRAL AMI Imaging System.

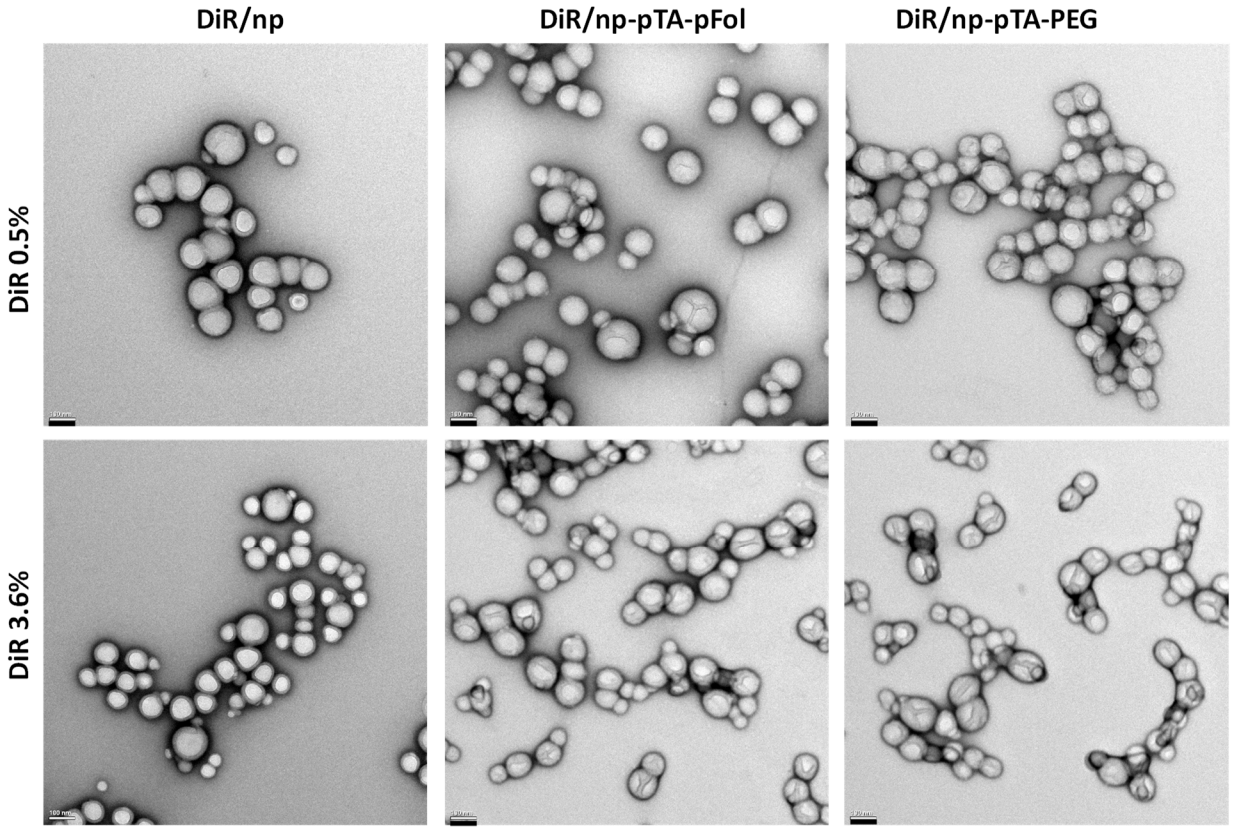

Figure S3. Transmission electron microscopy of NPs with different DiR loading. Scale bars: 100 nm.

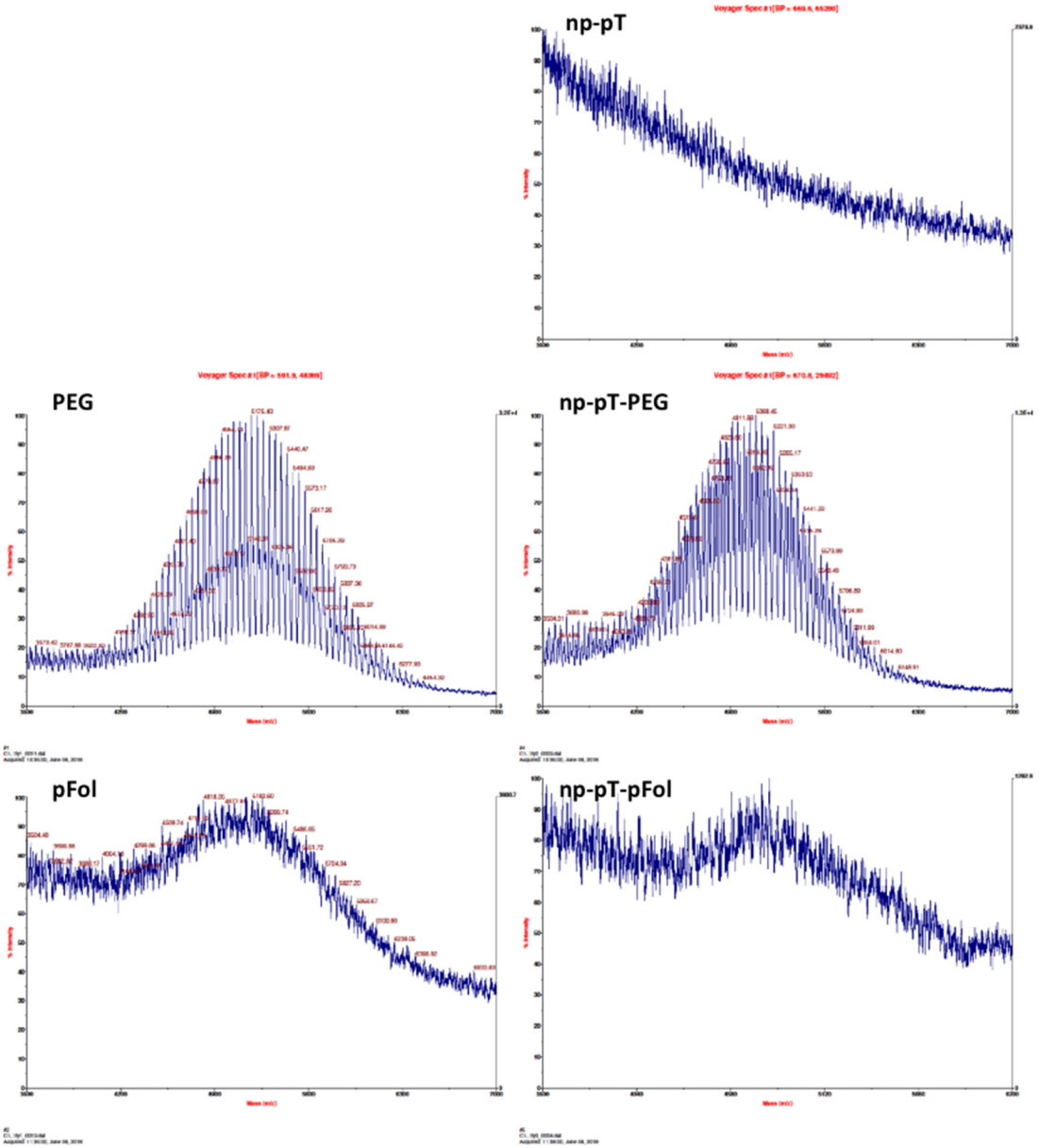

Figure S4. Matrix-assisted laser desorption/ionization mass spectrometry (MALDI-MS) of np-pT, PEG, np-pT-PEG, pFol, and np-pT-pFol.

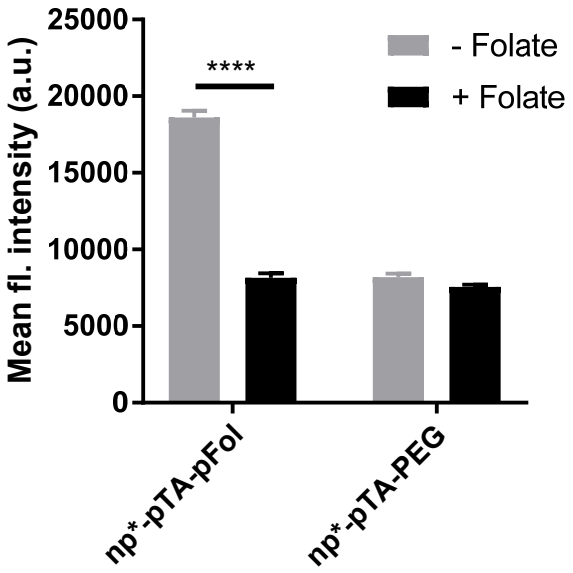

Figure S5. NP interaction with folate receptor-overexpressing KB cells in the absence (-Folate) and presence (+Folate) of extra folate (1 mM) in the culture medium. np*-pTA-pFol or np*-pTA-PEG: Rhodamine-labeled NPs decorated with pFol or mPEG *via* pTA. KB cells were incubated with the NPs for 2 h in the specified condition and analyzed by flow cytometry. n = 3 measurements of a representative batch (mean ± s.d.). ****: $p < 0.0001$ by Sidak's multiple comparisons test.

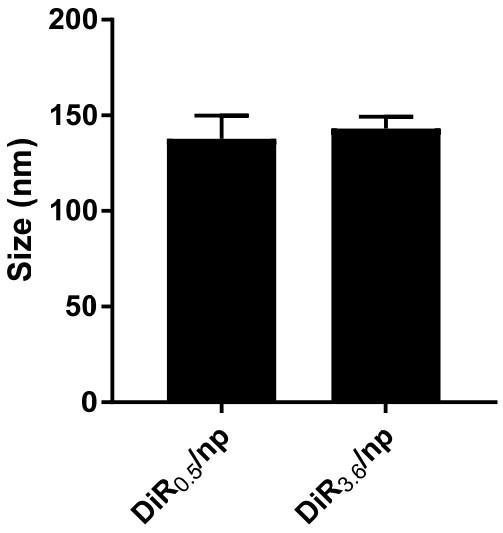

Figure S6. Average diameters of DiR/np in 50% FBS. $DiR_{0.5}$/np and $DiR_{3.6}$/np were dispersed in 50% FBS, and the size was measured by DLS. n = 3 independent batches (mean ± s.d.). No statistical difference by unpaired t-test.

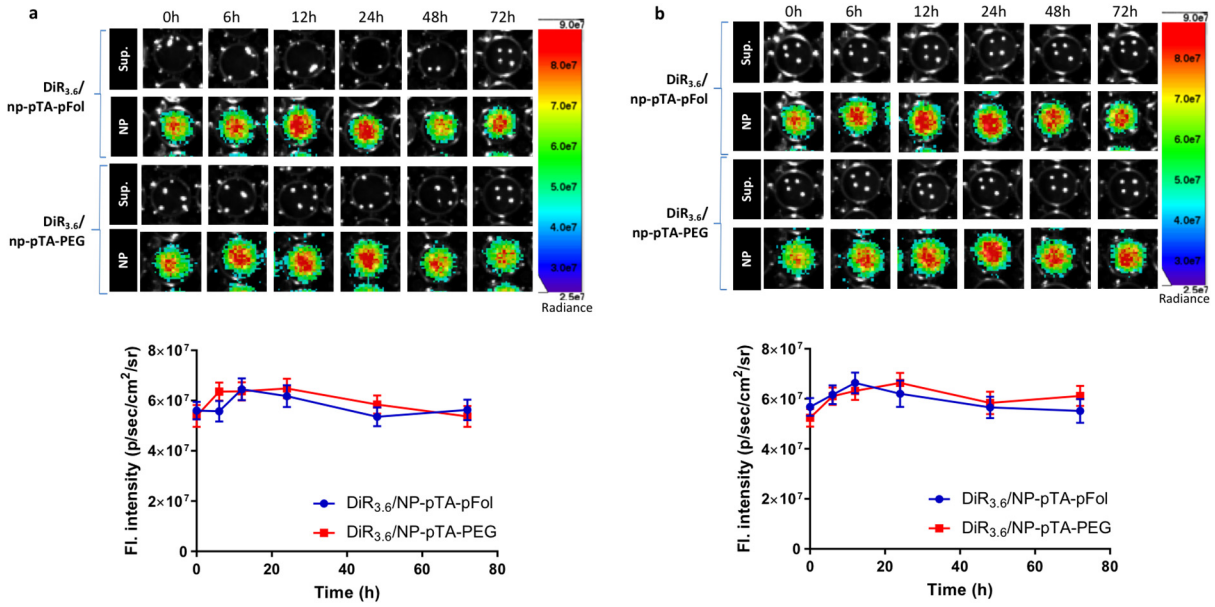

Figure S7. Stability of DiR3.6/np-pTA-pFol and DiR3.6/np-pTA-PEG in mouse serum (NPs: 1 mg/mL, DiR loading: 3.6%), measured twice (a, b) with NPs prepared independently and identically as the NPs shown in Fig. 1. Top: Fluorescence images of supernatants and NPs (redispersed in fresh mouse serum) collected at different time points during the incubation in mouse serum. Bottom: Fluorescence intensity of the NPs collected at the specified time points and redispersed in fresh mouse serum, quantified by the AMI viewer image software. Error bars: s.d. of 3 readings of the same sample.

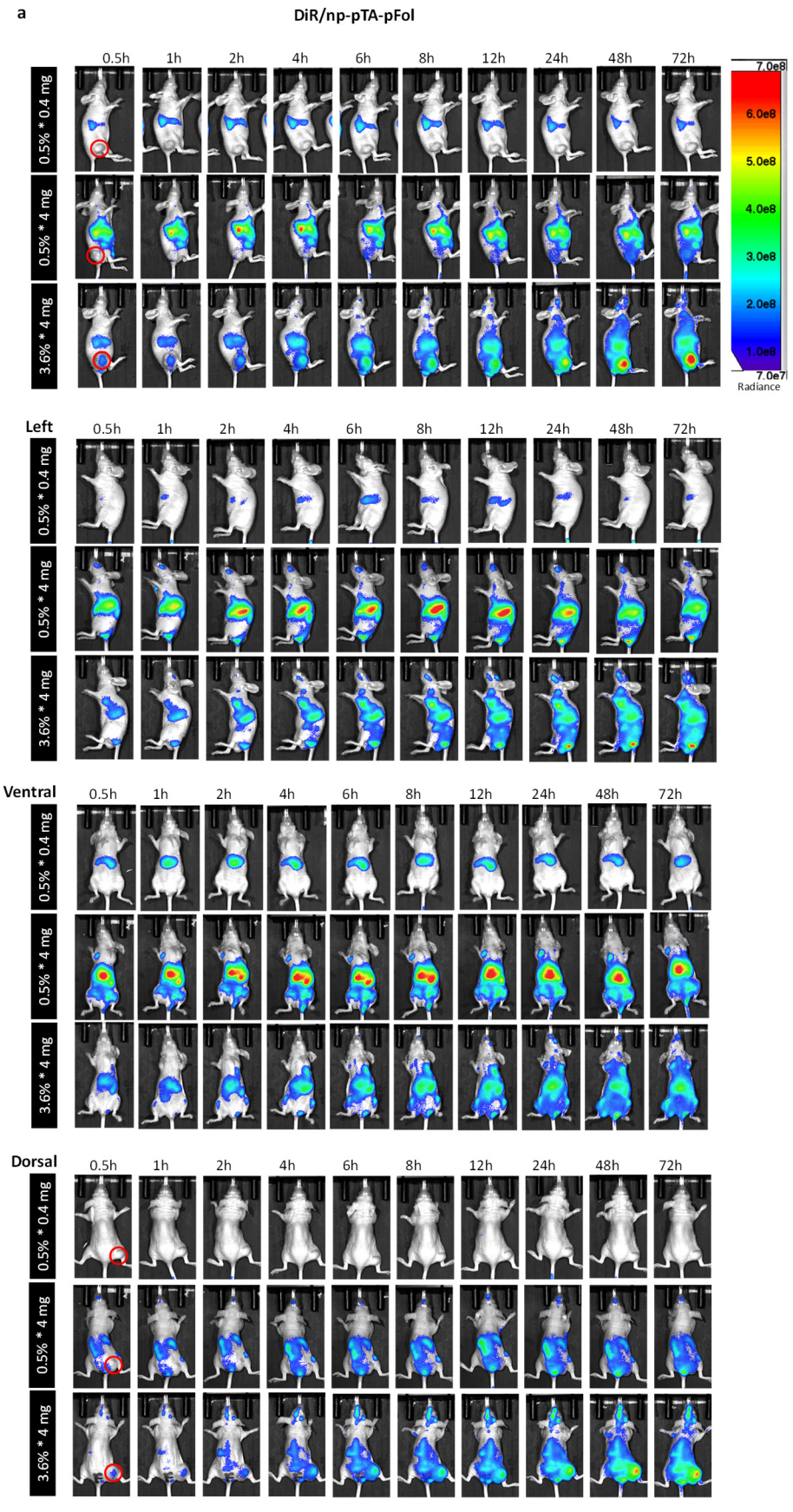
a
DiR/np-pTA-pFol
0.5h
1h
2h
4h
6h
8h
12h
24h
48h
72h
0.5% * 0.4 mg
0.5% * 4 mg
3.6% * 4 mg
7.0e8
6.0e8
5.0e8
4.0e8
3.0e8
2.0e8
1.0e8
7.0e7
Radiance
Left
Ventral
Dorsal

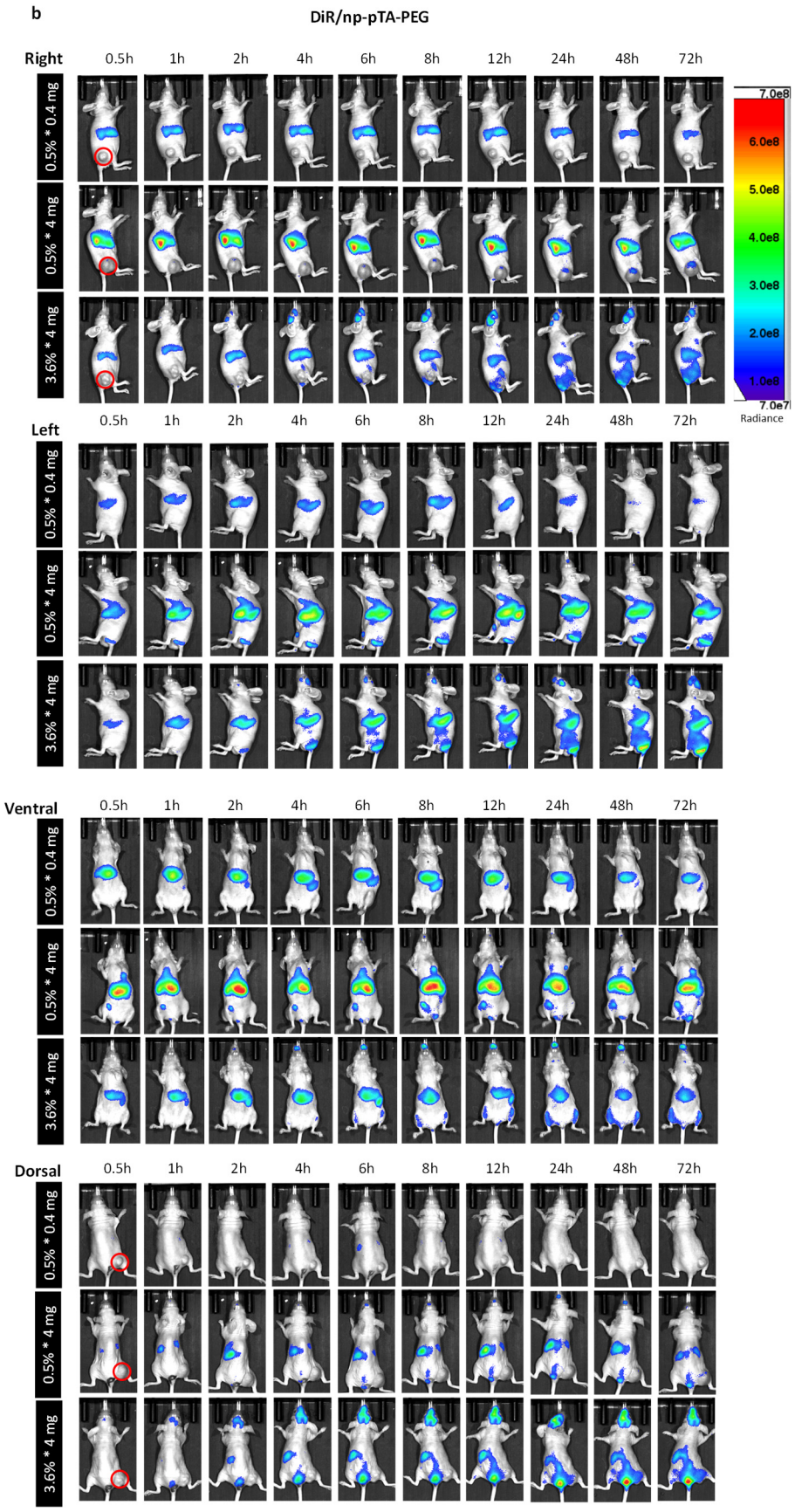
b
DiR/np-pTA-PEG
Right
Left
Ventral
Dorsal
0.5h
1h
2h
4h
6h
8h
12h
24h
48h
72h
0.5% * 0.4 mg
0.5% * 4 mg
3.6% * 4 mg
7.0e8
6.0e8
5.0e8
4.0e8
3.0e8
2.0e8
1.0e8
7.0e7
Radiance

Figure S8. Real-time whole body imaging of KB tumor-bearing female nude mice at different time points after tail vein injection of (a) DiR/np-pTA-pFol or (b) DiR/np-pTA-PEG with different DiR loading (0.5 or 3.6%) at NP doses of 0.4 or 4 mg per mouse (Fig. 2). Red solid circles indicate subcutaneous KB tumors.

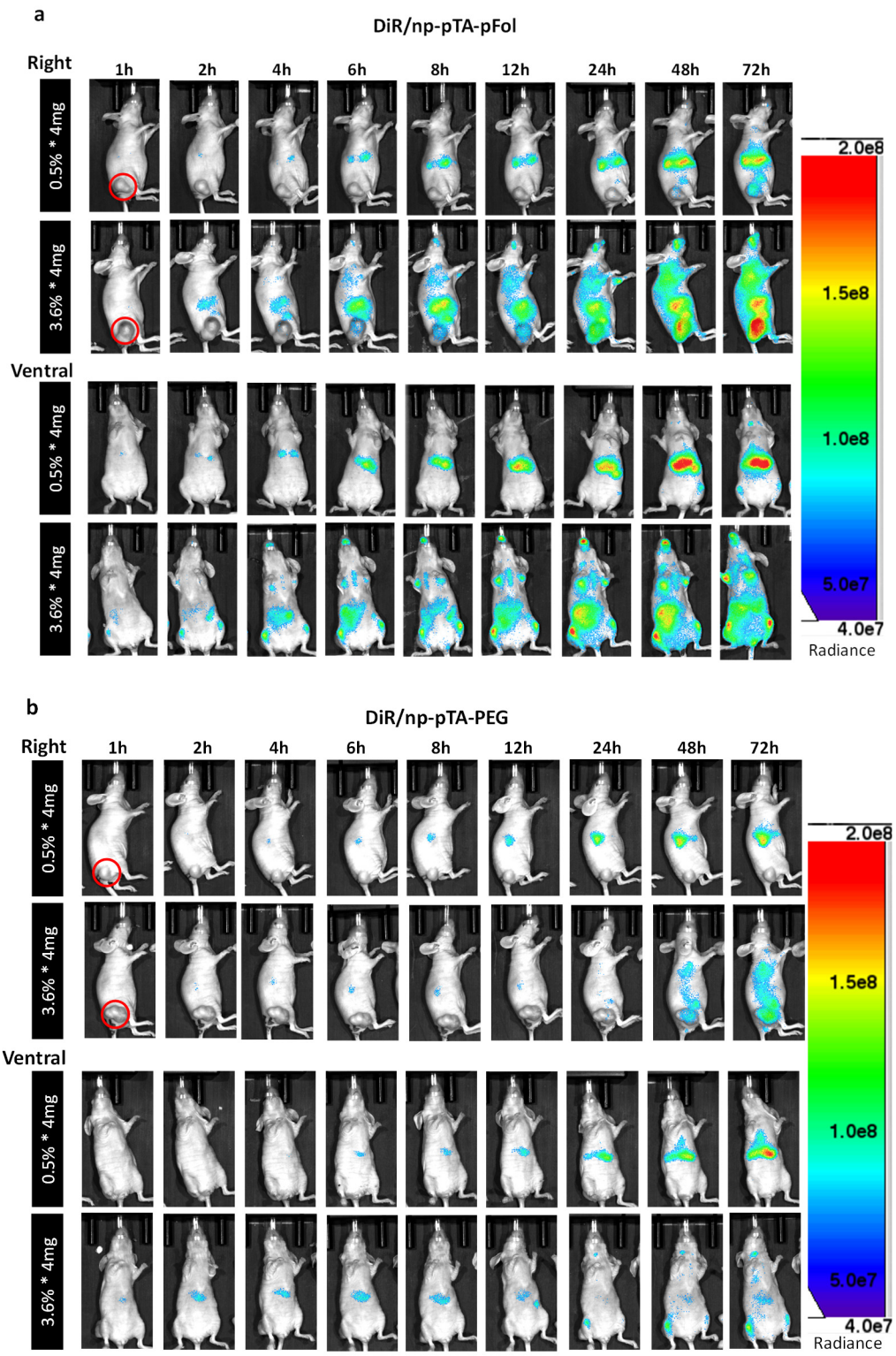

Figure S9. Real-time whole body imaging of KB tumor-bearing female nude mice at different time points after tail vein injection of (a) DiR/np-pTA-pFol or (b) DiR/np-pTA-PEG with different DiR loading (0.5 or 3.6%) at a NP dose of 4 mg per mouse. Red solid circles indicate subcutaneous KB tumors.

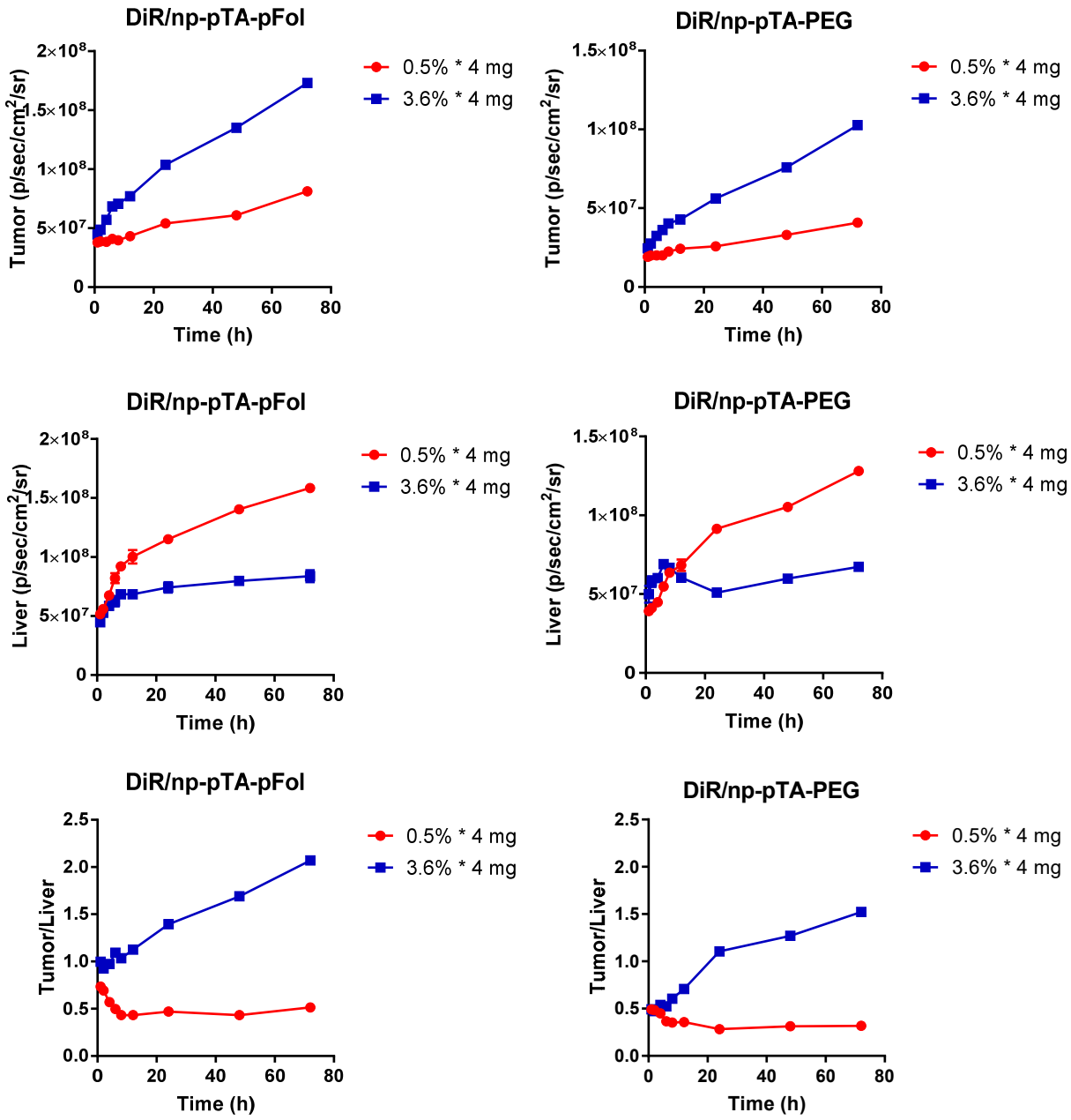

Figure S10. Fluorescence intensity of tumor and liver *in situ* and their ratio after tail vein injection of (left) DiR/np-pTA-pFol or (right) DiR/np-pTA-PEG (**Figure S9**). The fluorescence intensity of region of interest (ROI) was quantified by the AMI viewer image software and expressed as radiance (p/sec/cm^2/sr).

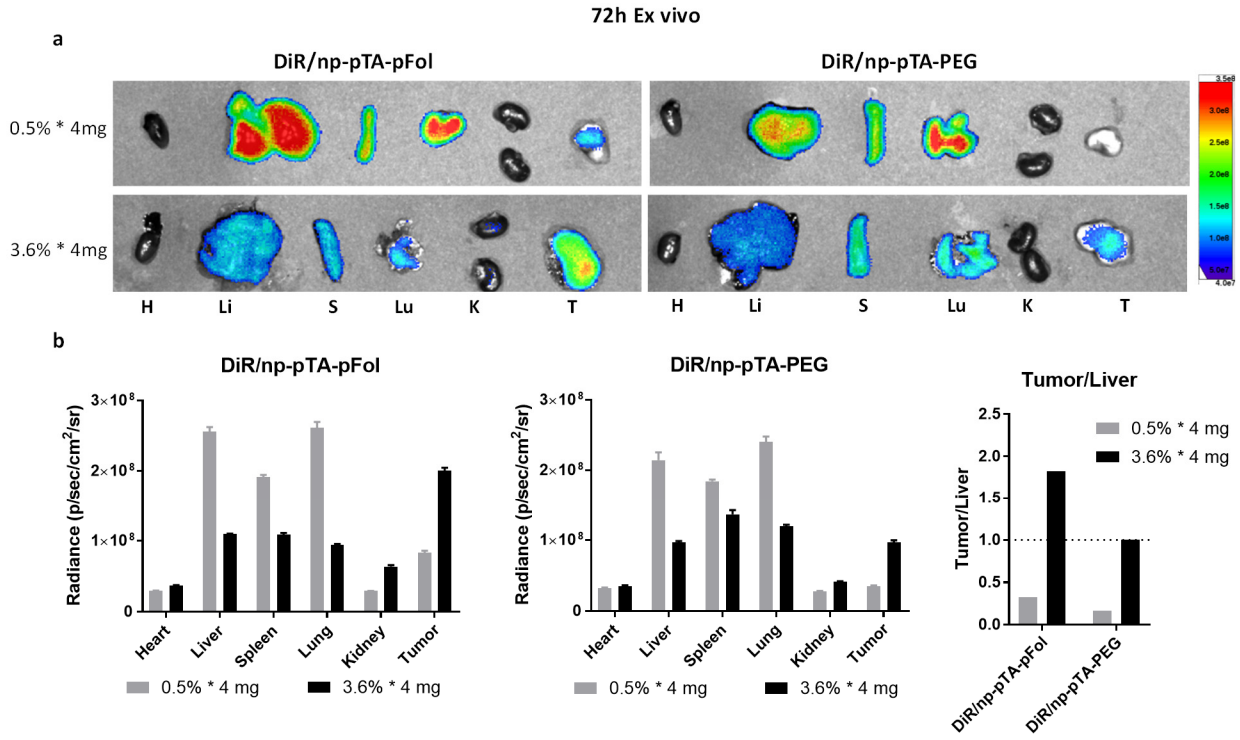

Figure S11. (a) Fluorescence images, (b) signal intensity of major organs and tumor/liver ratio of the signals acquired *ex vivo* at 72 h post-injection of DiR/np-pTA-pFol or DiR/np-pTA-PEG (**Figure S9**). H: heart; Li: liver; S: spleen; Lu: lung; K: kidneys; T: KB tumor. The fluorescence intensity of ROI was quantified by the AMI viewer image software and expressed as radiance (p/sec/cm^2/sr). Error bars: s.d. of 3 readings of the same subject.

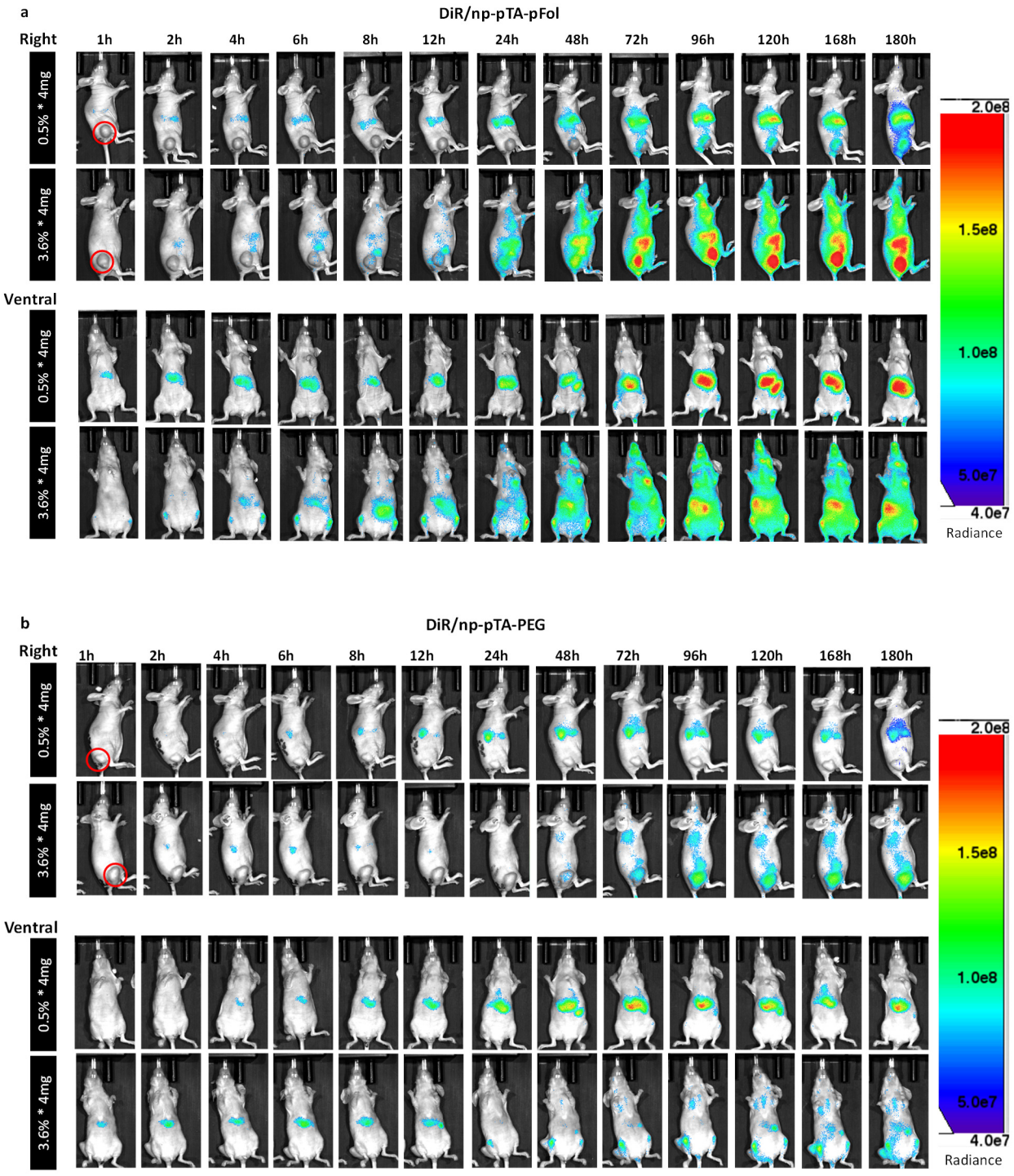

Figure S12. Real-time whole body imaging of KB tumor-bearing female nude mice at different time points after tail vein injection of (a) DiR/np-pTA-pFol or (b) DiR/np-pTA-PEG with different DiR loading (0.5 or 3.6%) at a NP dose of 4 mg per mouse. Red solid circles indicate subcutaneous KB tumors.

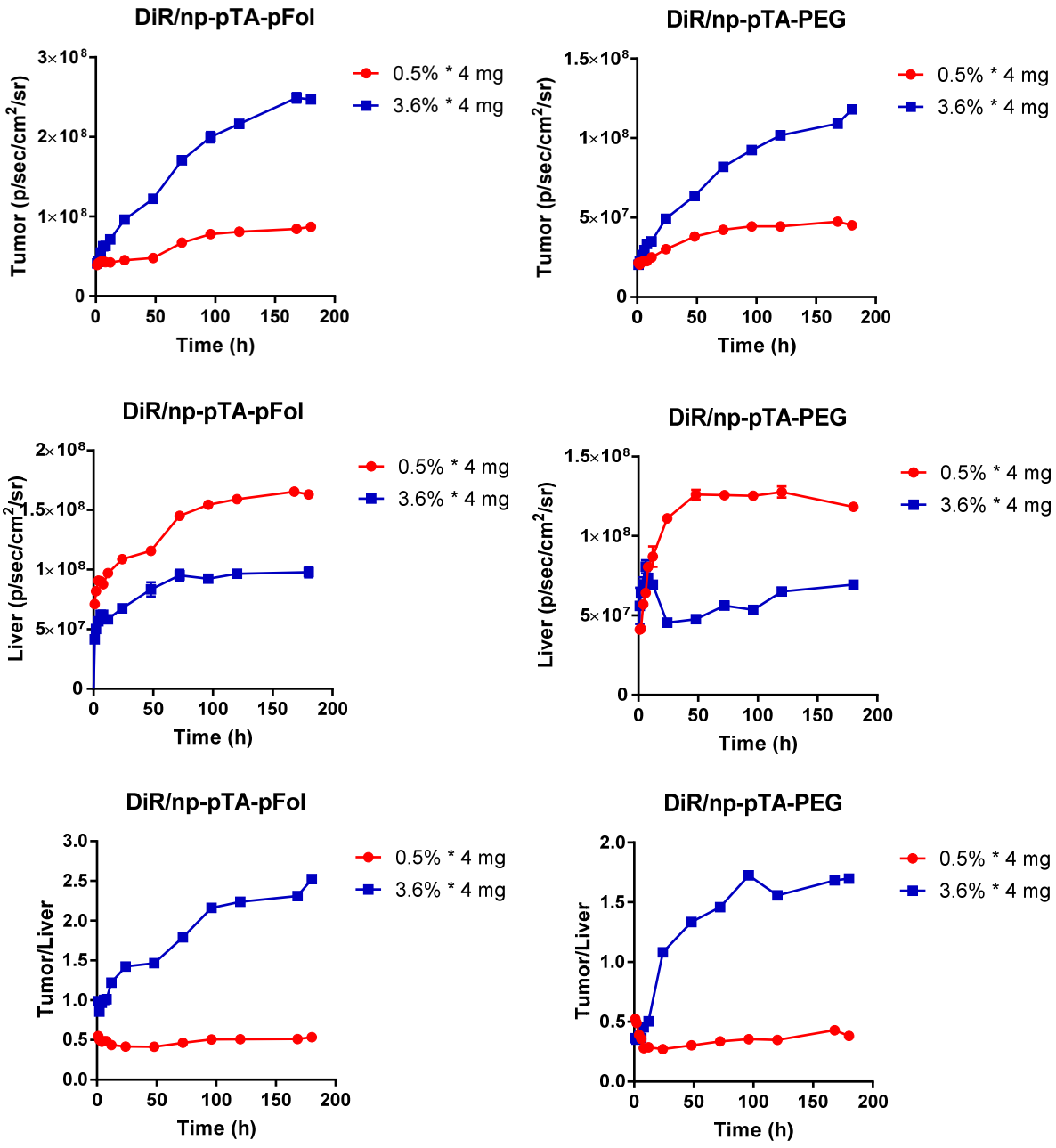

Figure S13. Fluorescence intensity of tumor and liver *in situ* and their ratio after tail vein injection of (left) DiR/np-pTA-pFol or (right) DiR/np-pTA-PEG (**Figure S12**). The fluorescence intensity of ROI was quantified by the AMI viewer image software and expressed as radiance (p/sec/cm^2/sr).

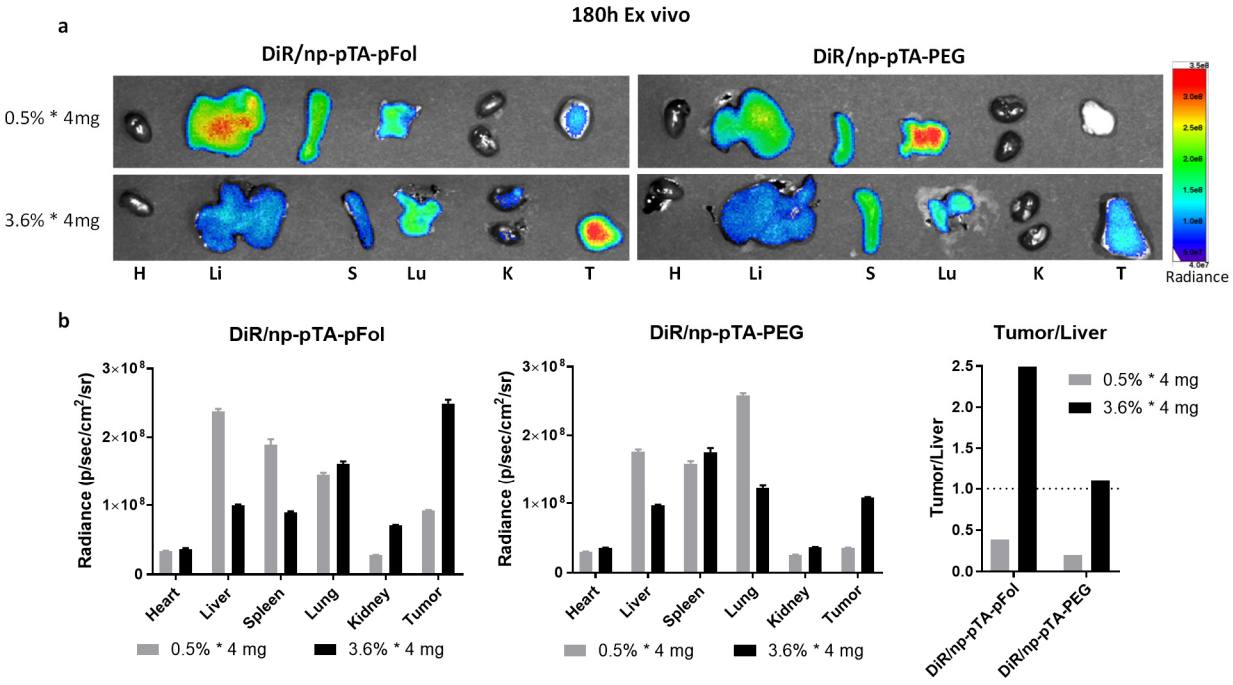

Figure S14. (a) Fluorescence images, (b) signal intensity of major organs and tumor/liver ratio of the signals acquired *ex vivo* at 180 h post-injection of DiR/np-pTA-pFol or DiR/np-pTA-PEG (**Figure S12**). H: heart; Li: liver; S: spleen; Lu: lung; K: kidneys; T: KB tumor. The fluorescence intensity of ROI was quantified by the AMI viewer image software and expressed as radiance (p/sec/cm^2/sr). Error bars: s.d. of 3 readings of the same subject.

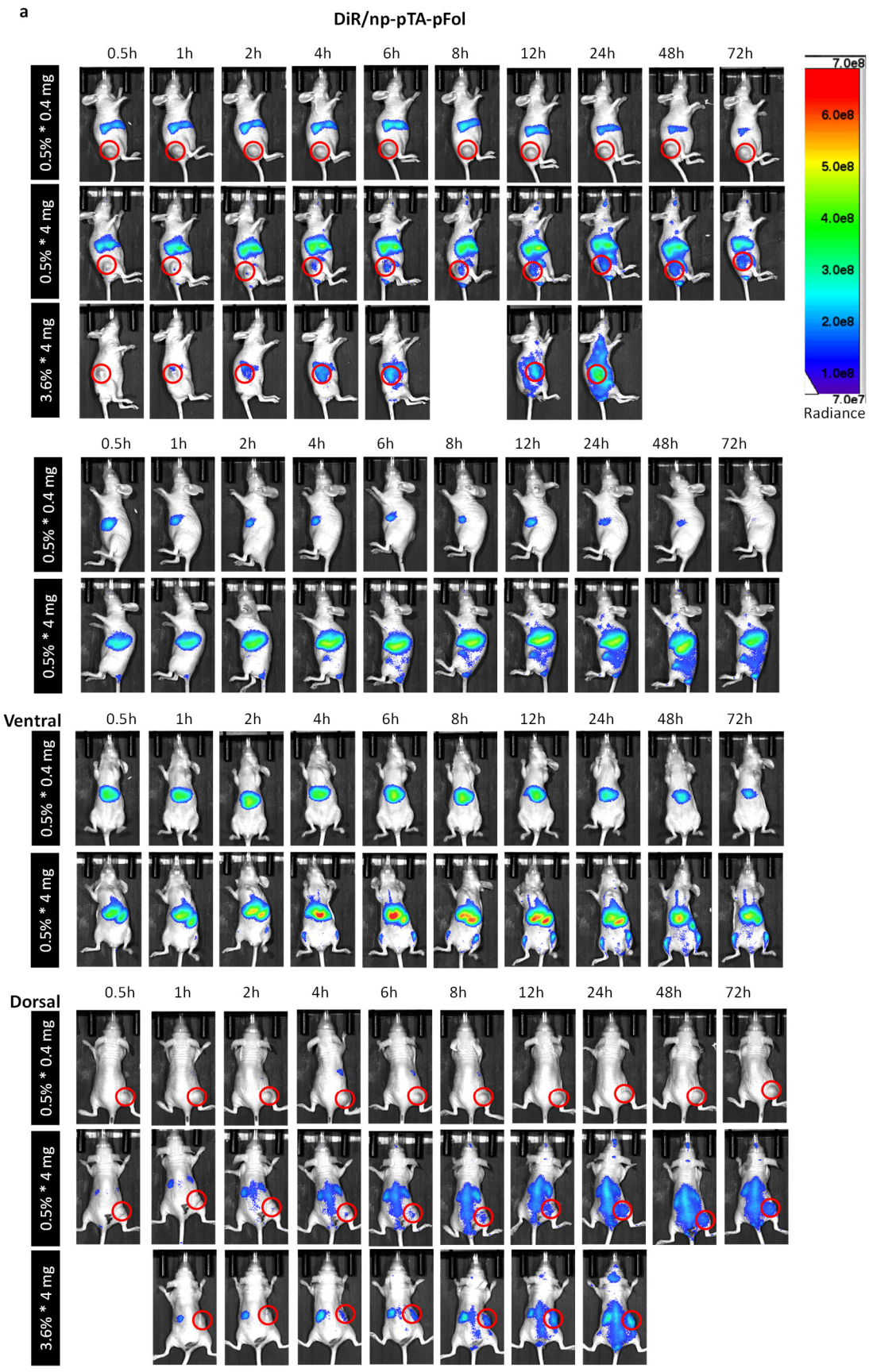
a
DiR/np-pTA-pFol
0.5h
1h
2h
4h
6h
8h
12h
24h
48h
72h
0.5% * 0.4 mg
0.5% * 4 mg
3.6% * 4 mg
7.0e8
6.0e8
5.0e8
4.0e8
3.0e8
2.0e8
1.0e8
7.0e7
Radiance
Ventral
Dorsal

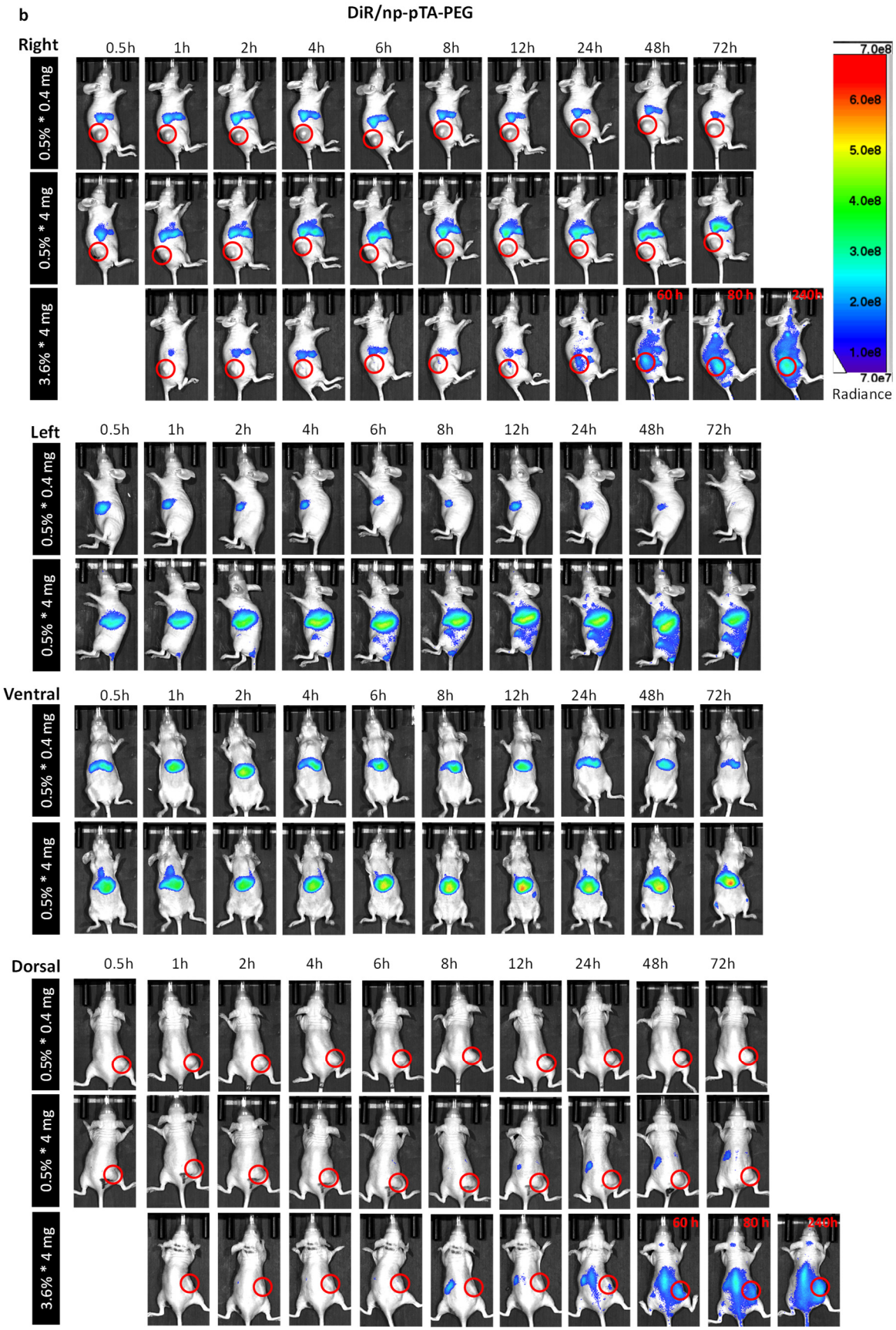
b
DiR/np-pTA-PEG
Right
0.5h
1h
2h
4h
6h
8h
12h
24h
48h
72h
0.5% * 0.4 mg
0.5% * 4 mg
3.6% * 4 mg
60 h
80 h
240h
7.0e8
6.0e8
5.0e8
4.0e8
3.0e8
2.0e8
1.0e8
7.0e7
Radiance
Left
Ventral
Dorsal

Figure S15. Real-time whole body imaging of KB tumor-bearing female nude mice at different time points after tail vein injection of (a) DiR/np-pTA-pFol or (b) DiR/np-pTA-PEG with different DiR loading (0.5 or 3.6%) at NP doses of 0.4 or 4 mg per mouse. Red solid circles indicate subcutaneous KB tumors.

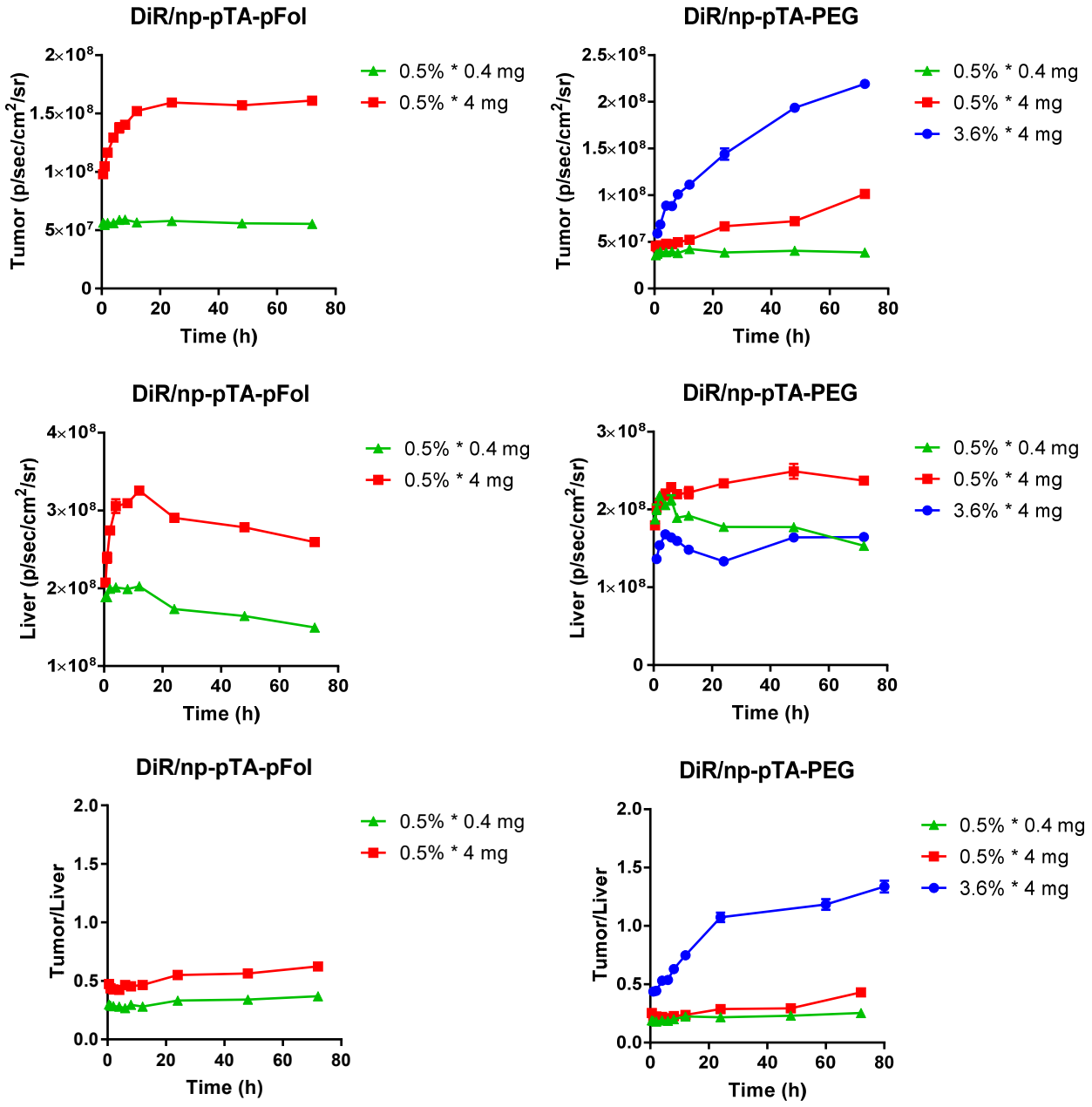

Figure S16. Fluorescence intensity of tumor and liver *in situ* and their ratio after tail vein injection of (left) DiR/np-pTA-pFol or (right) DiR/np-pTA-PEG (**Figure S15**). The fluorescence intensity of ROI was quantified by the AMI viewer image software and expressed as radiance (p/sec/cm^2/sr).

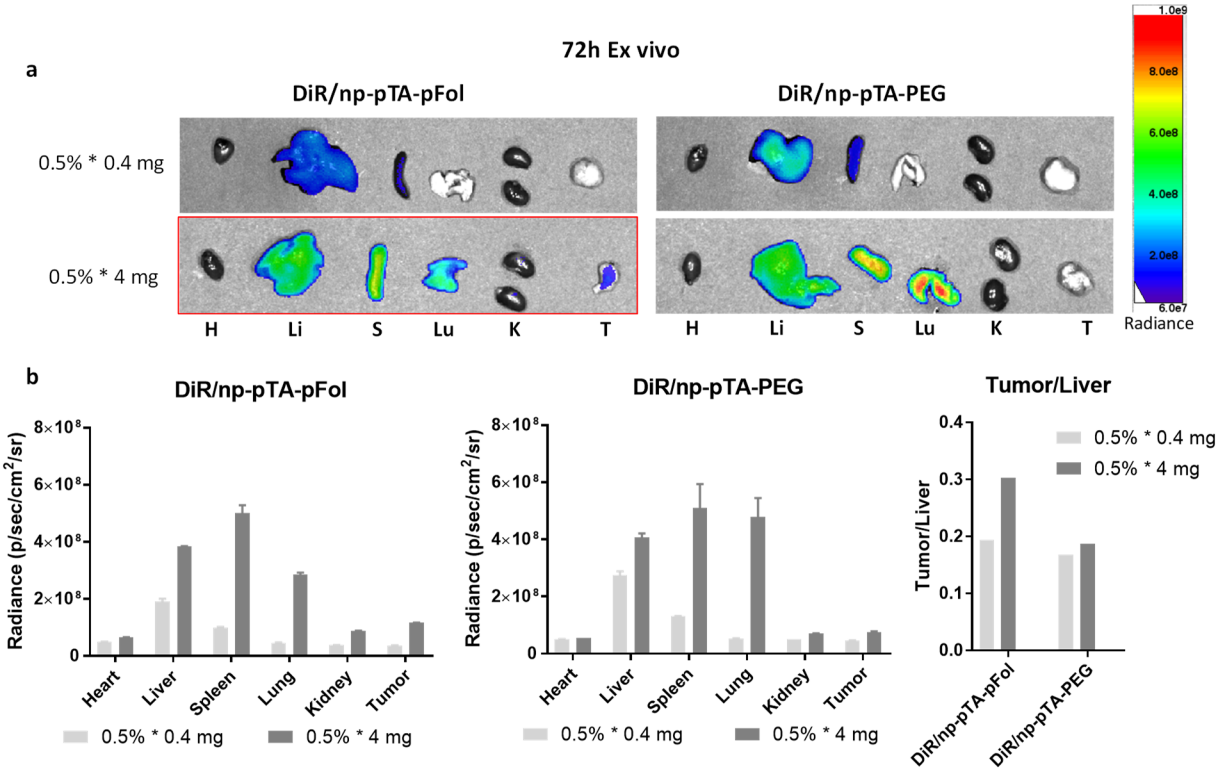

Figure S17. (a) Fluorescence images, (b) signal intensity of major organs and tumor/liver ratio of the signals acquired *ex vivo* at 72 h post-injection of DiR/np-pTA-pFol or DiR/np-pTA-PEG (**Figure S15**). H: heart; Li: liver; S: spleen; Lu: lung; K: kidneys; T: KB tumor. The fluorescence intensity of ROI was quantified by the AMI viewer image software and expressed as radiance (p/sec/cm^2/sr). Error bars: s.d. of 3 readings of the same sample.

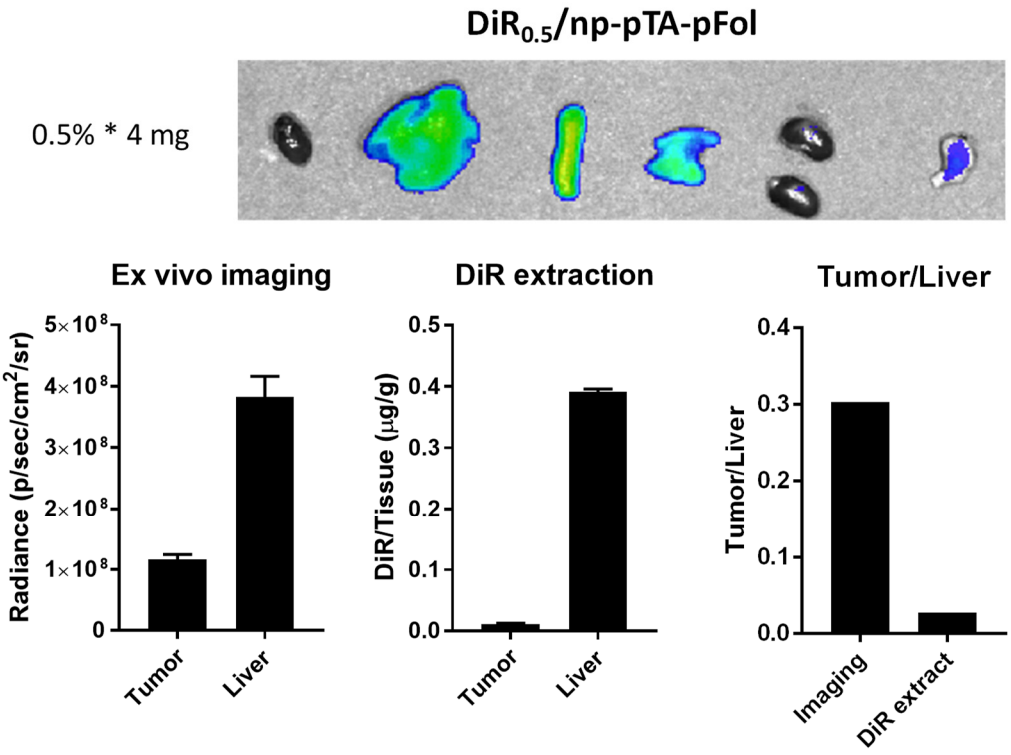

Figure S18. Comparison of fluorescence signals of tumor and liver and their ratios quantified by *ex vivo* fluorescence image analysis and by liquid-liquid extraction (**Figure S15**). Images and organ samples were obtained from a mouse receiving 4 mg of $DiR_{0.5}$/np-pTA-pFol at 72 h after tail vein injection. Error bars: s.d. of 3 readings of the same subject.

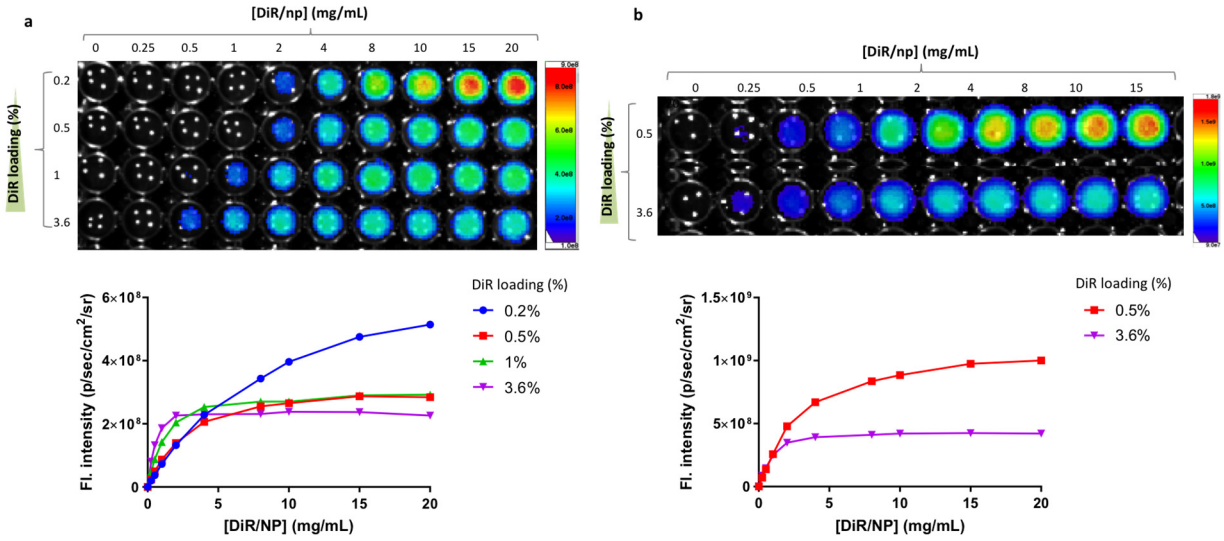

Figure S19. Fluorescence intensity *vs*. concentration of DiR-loaded PLGA NPs (DiR/np) with different dye loading, measured with (a) the same batch of NPs as Fig. 6 and (b) an independently prepared batch of NPs. Top: Fluorescence images of DiR/np at different concentrations shown on the right. Bottom: The fluorescence intensity was quantified by the SPECTRAL AMI Imaging System.

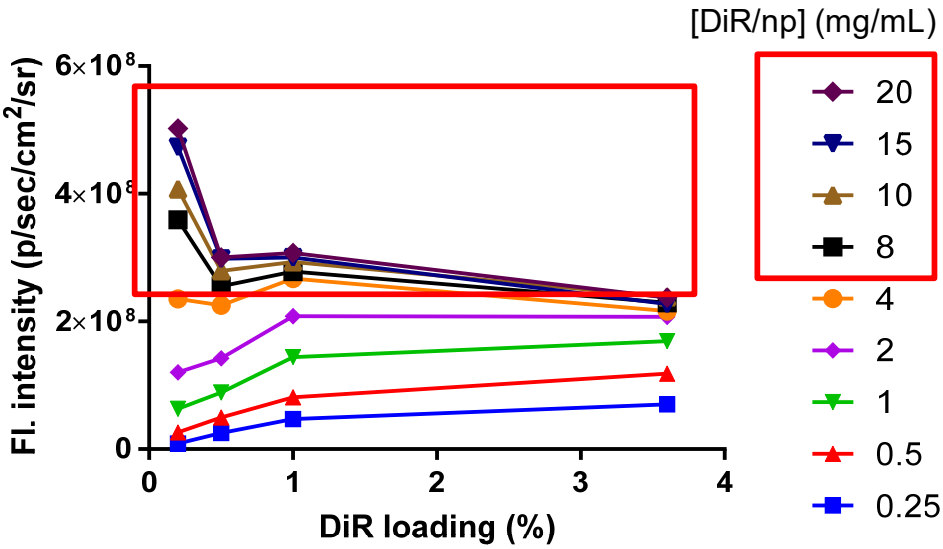

Figure S20. Fluorescence intensity *vs*. DiR loading of DiR/np at different NP concentrations (replotted from Fig. 6a). DiR/np with different DiR loading were suspended in mouse serum at the indicated concentrations, and the fluorescence intensity was quantified by the AMI viewer image software.

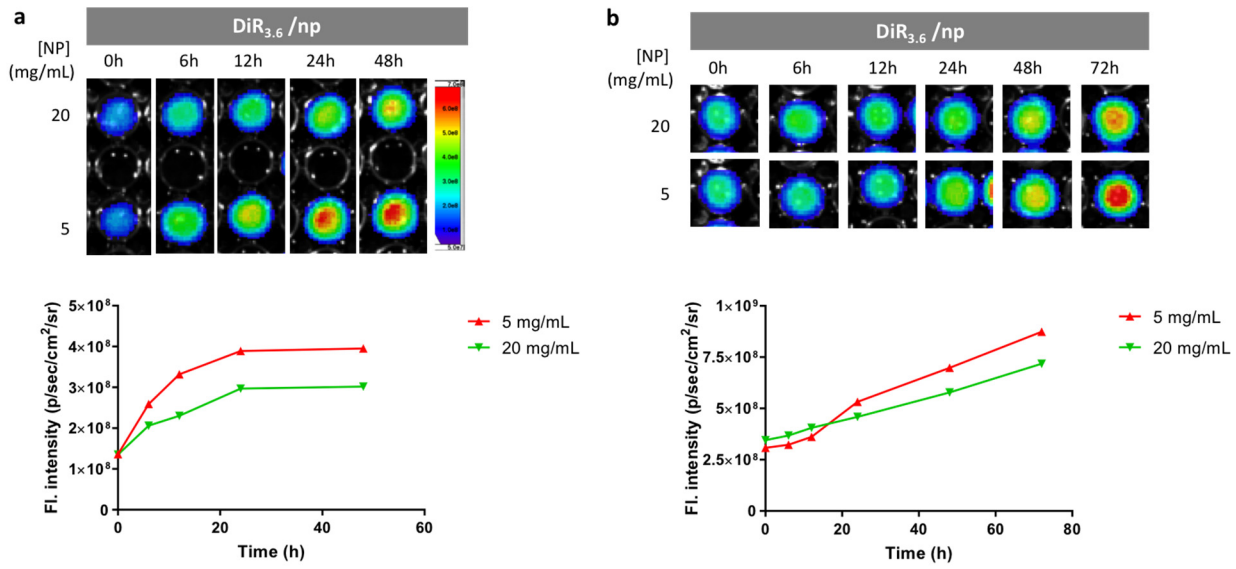

Fig. 21. Fluorescence intensity of $DiR_{3.6}$/np suspended in mouse serum at different NP concentrations, observed at different time points. (a, b) Measurements with two independently prepared batches of NPs. The fluorescence intensity was quantified by the SPECTRAL AMI Imaging System.

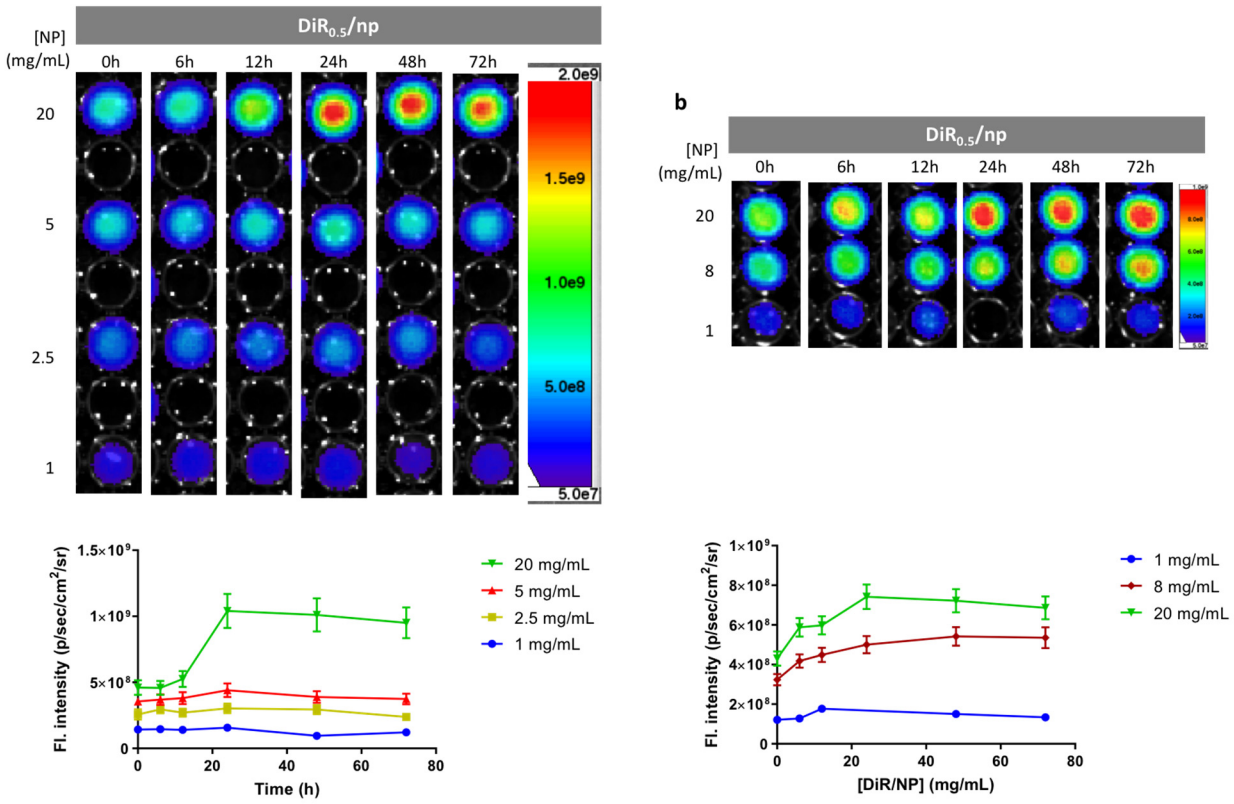

Fig. 22. Fluorescence intensity of $DiR_{0.5}$/np suspended in mouse serum at different NP concentrations, observed at different time points. (a, b) Measurements with two independently prepared batches of NPs. The fluorescence intensity was quantified by the SPECTRAL AMI Imaging System. Error bars: s.d. of 3 readings of the same sample.

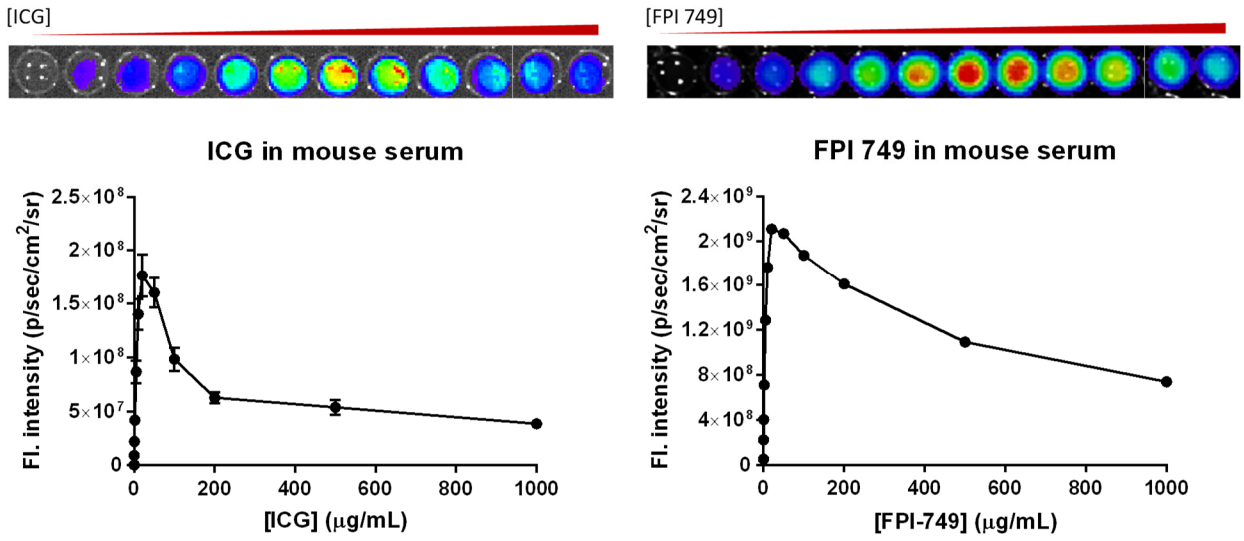

Figure S23. Fluorescence intensity *vs*. concentration of free ICG and FPI 749 (equivalent to Cy7) in mouse serum. The fluorescence intensity of ICG was quantified by the IVIS Lumina II Optical Imaging System with an excitation wavelength of 745 nm and an emission filter for ICG. FPI 749 was detected by the SPECTRAL AMI Imaging System with an excitation and emission wavelength of 745 and 790 nm.